ACS APPLIED MATERIALS & INTERFACES

Research Article

www.acsami.org

Facile Fabrication of Gold Nanoparticles-Poly(vinyl alcohol) Electrospun Water-Stable Nanofibrous Mats: Efficient Substrate Materials for Biosensors

Juan Wang,[†,‡] Hong-Bin Yao,[†] Dian He,[†] Chuan-Ling Zhang,[†] and Shu-Hong Yu*[,†]

[†]Division of Nanomaterials and Chemistry, Hefei National Laboratory for Physical Sciences at Microscale, Department of Chemistry, National Synchrotron Radiation Laboratory, University of Science and Technology of China, Hefei, Anhui 230026, P. R. China

[‡]Department of Chemistry and Chemical Engineering, Huainan Normal University, Huainan, Anhui 232001, P. R. China

ABSTRACT: Electrospun nanofibrous mats are intensively studied as efficient scaffold materials applied in the fields of tissue engineering, catalysis, and biosensors due to their flexibility and porosity. In this paper, we report a facile route to fabricate gold nanoparticles-poly(vinyl alcohol) (Au NPs-PVA) hybrid water stable nanofibrous mats with tunable densities of Au NPs and further demonstrate the potential application of as-prepared Au NPs-PVA nanofibrous mats as efficient biosensor substrate materials. First, through the designed in situ cross-linkage in coelectrospun PVA-glutaraldehyde nanofibers, water insoluble PVA nanofibrous mats with suitable tensile strength were successfully prepared. Then, 3-mercaptopropyltrimethoxysilane (MPTES) was modified on the surface of obtained PVA nanofibrous films, which triggered successful homogeneous decoration of Au NPs through gold−sulfur bonding interactions. Finally, the Au NPs-PVA nanofibrous mats embedded with horseradish peroxidase (HRP) by electrostatic interactions were used as biosensor substrate materials for H_2O_2 detection. The fabricated HRP-Au NPs/PVA biosensor showed a highly sensitive detection of H_2O_2 with a detection limit of 0.5 μM at a signal-to-noise ratio of 3. By modifying other different functional nanaoparticles or enzyme on the PVA nanofibrous film will further expand their potential applications as substrate materials of different biosensors.

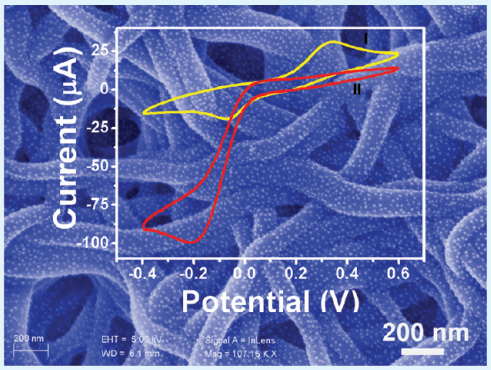

KEYWORDS: *electrospun PVA nanofibers, cross-link, water stable, Au nanoparticles, H_2O_2 detection, biosensors*

1. INTRODUCTION

Two dimensional mat materials that are constructed by micro- or nano-fibers are intensively applied as substrate materials in the fabrication of advanced intelligent devices due to their flexibilities, high specific surface area, high porosity, and good mechanical strength.[1−3] As a facile and versatile method to prepare fiber fabrics, electrospinning has been broadly used to generate various synthetic and natural polymer fibers with a small diameter ranging from tens of nanometers to a few micrometers.[4−7] The electrospinning technical process involves the formation of a liquid jet of polymer solution induced by a high voltage (1−30 kV), stretch of polymer jet, and collection of fiber on the counter electrode. The obtained electrospun fibrous mats with macroscales are easily handled and could be applied in fields as diverse as optoelectronics,[8,9] catalyst,[10] filtration,[11,12] protective clothing,[1,13] tissue engineering scaffolds,[7,14,15] and biosensors.[16−18]

Among a wide series of electrospinnable polymers, poly(vinyl alcohol) (PVA) attracted particular attention due to its plenty advantageous properties such as water solubility, hydrophilicity, chemical stability, and biocompatibility.[19−21] The electrospinning process of PVA has been comprehensively studied, in which the influence of parameters of PVA, e.g., pH value,[22] molecular weight,[23] and degrees of hydrolysis,[19] on the formation of electrospun fibers have been investigated. In order to really realize the practical applications of an electrospun PVA fibrous mat, its water stability is a vital factor that should be addressed.[21,24] The cross-linking role of PVA on the increase of water insolubility has been introduced in the electrospun PVA fiber mat.[25] The thermal and photo induced cross-linking processes of PVA/poly(acrylic acid) modified electrospun fibers resulting in water insoluble fibrous mats have been reported.[21,26]

In particular, the chemical cross-linking induced by glutaraldehyde (GA), during which the hydroxyl groups of the PVA and the aldehyde groups of GA react in the presence of a strong acid, has also been considered to enhance the water stability of PVA.[27] Through exposing the electrospun PVA fibrous mat to GA and a strong acid in solution with a nonsolvent for PVA or GA and strong acid vapors, the *ex situ* cross-linking of PVA triggered by GA occurred on the surface of PVA fibers rendering the water insoluble to a PVA fibrous

Received: December 11, 2011
Accepted: March 12, 2012
Published: March 12, 2012

mat.[28] Recently, the concept that the *in situ* cross-linked process in electrospun fibers containing both PVA as backbones and GA as cross-linking agents have been introduced to generate water insoluble PVA fibrous mats.[29] The electrospun PVA fibrous mats yielded by this method displayed outstanding water insolubility, and the uniform fiber morphology can be maintained after soaking in water overnight.

Besides the water stability of the electrospun PVA fibrous mat, its functionalization is also necessary to be considered as its ultimate goal for the fabrication of functional devices.[2,21,24,28,30] Noble metal nanoparticles exhibit rich optical and electronic properties in addition to their pronounced biocompatibility, which therefore have been immobilized into or onto substrate materials for nanomedicine,[31] drug and gene delivery,[32] and biosensor.[33,34] Recently, the synthesis and assembly of noble metal nanoparticles on electrospun nanofibers via chemical modification for producing functional nanocomposites have attracted much attention.[35−37] Specifically, on water stable electrospun PVA nanofibers, gold nanoparticles were immobilized for catalytic applications.[38] Our group has successfully incorporated silver nanoparticles into electrospun PVA nanofibers to fabricate a free-standing and flexible surface-enhanced Raman scattering substrate material.[2]

In this paper, we present efficient free-standing biosensor substrate materials prepared by decorating functional Au nanoparticles on water stable electrospun PVA nanofibrous mats, which can combine the flexible and portable properties of PVA mats and biorelated functions of Au nanoparticles together. The potential application as a biosensor substrate material of the obtained Au NPs-PVA hybrid nanofibrous water stable mats was demonstrated by immobilizing the horseradish peroxidase (HRP) onto the mat for H_2O_2 detection. The fabricated HRP-Au NPs/PVA nanofibrous mat biosensor can realize the highly sensitive detection of H_2O_2 exhibiting fast response, broad linear range, and low detection limit compared with previous biosensors fabricated by other methods.[39−41] On the other hand, the obtained substrate can be tailored freely due to the flexibility and free-standing feature of the electrospun polymer nanofibrous mat. Combined with the low-cost and high-throughput of the electrospinning progress, the water-stable Au NPs-PVA hybrid nanofibrous substrate material for H_2O_2 detection shows significant benefits such as high sensitivity, stability, reusability, cheap, and portable features. Furthermore, many other enzymes can immobilize on the Au NPs-PVA hybrid nanofibrous films as well for their wide applications in bioelectroanalysis and bioelectrocatalysis.

2. EXPERIMENTAL SECTION

2.1. Materials. PVA powder and GA aqueous solution (25 wt%) was purchased from Aldrich. Sodium citrate, hydrochloroauric acidtrihydrate ($HAuCl_4{\cdot}3H_2O$, 99.9%), and hydrogen peroxide (30 wt %) was purchased from Beijing Chemical Reagents Co., Ltd. (China). Horseradish peroxidase (HRP, RZ ∼ 3, activity ≥ 250 units mg^{-1}) was purchased from Sangon Biotech (ShangHai) Co., Ltd. Hydroquinone (HQ) was purchased from Sinopharm Chemical Reagent Co., Ltd. (China). Silane coupling agent 3-mercaptopropyltrimethoxysilane (MPTES) was obtained from Chemwish Technology Co. Ltd. (Wuhan). The solutions used for electrochemical characterization were freshly prepared using 0.1 M of phosphate buffer (PB, pH 6.8) unless otherwise noted. All the reagents were analytical grade and used as received without further purification.

2.2. Preparation of Water-Stable PVA Fibrous Mat. PVA solution (8 wt %) was prepared by dissolving PVA powder into deionized water (DIW) at 95 °C overnight under magnetic stirring, and then the solution was cooled down to room temperature naturally. Subsequently, the GA solution was added to PVA aqueous solution under vigorous stirring to achieve a homogeneous viscoelastic spinnable solution, in which the mass ratio of PVA and GA was 4:1. The electrospinning of PVA/GA solution was carried out at ambient temperature using a syringe with a needle having an inner diameter of 0.8 mm at an applied voltage of 9 kV. The feeding rate and the tip to collector distance were set to be 0.3 mL/h and 17 cm, respectively. Freshly prepared PVA/GA nanofibrous mats were cross-linked upon an acid treatment by immersed in a mixed solution containing 10 vol % of HCl aqueous solution (37 wt %) and 90 vol % methanol for the desired time to produce water-stable nanofibrous mats.

2.3. Synthesis of Au NPs. An Au NPs aqueous solution was prepared according to a previously reported method.[42] Typically, 4 mL of 1 wt % $HAuCl_4$ aqueous solution was diluted into 100 mL of DIW in a flask. Then, the diluted $HAuCl_4$ aqueous solution was heated to 130 °C for refluxing under constant stirring. After refluxing for 15 min, 12 mL of 1 wt % sodium citrate aqueous solution was added into aqueous $HAuCl_4$ quickly and kept refluxing for a further 5 min to form homogeneous Au NPs in aqueous solution. The obtained Au NPs aqueous solution was transfered into a beaker after cooling to room temperature and stored at 4 °C in a refrigerator before use.

2.4. Decoration of Au NPs on the Water-Stable PVA Fibrous Mat. The water-stable nanofibrous mats were immersed into the 3-mercaptopropyltrimethoxysilane (MPTES) ethanol solution (10 wt %) by vigorous shaking in an incubator shaker at 36.6 °C for 10 h and then rinsed with DIW and ethanol three times. The freshly washed nanofibrous mats were immersed into the desired volume of Au NPs aqueous solution (Au NPs concentration, 0.16 mg/mL; citrate concentration, 0.075 mg/mL) followed by vigorous shaking in an incubator shaker at 36.6 °C for 4 h until the Au NPs aqueous solution changed from red wine color to colorless. The as-produced Au NPs-decorated nanofibrous mats were rinsed with DIW three times, followed by drying at room temperature for 2 h, and stored under ambient conditions before use.

2.5. Preparation of Biosensor for H_2O_2 Detection. Prior to the preparation procedure of the biosensor, the glassy carbon electrode (GCE) with a diameter of 3 mm was polished carefully using an alumina slurry as a polisher to get a mirror-like surface followed by rinsing with DIW and ethanol and then drying by nitrogen. A water stable Au NPs-PVA fibrous mat was incubated with 3 mg/mL of HRP solution (1 mL) at 4 °C overnight in a humidity chamber. Then, the Au NPs-PVA fibrous mat modified by HRP was glued by Nafion aqueous solution (1 wt %) on the pretreated GCE and left to dry at room temperature. The modified electrode was washed gently with DIW three times and then soaked in PB at 4 °C. This modified electrode is denoted as HRP/Au NPs-PVA/GCE. The control sample, HRP/PVA/GCE was fabricated using similar procedures for the preparation of HRP/Au NPs-PVA/GCE including the incubation of cross-linked PVA mats with 3 mg/mL of HRP solution (1 mL) and following deposition on the GCE by glue Nafion (1 wt %). All the modified electrodes were stored at 4 °C in a refrigerator before use.

2.6. Electrochemical Measurement. Electrochemical experiments were carried by using a three-electrode system on an IM6ex electrochemical workstation (Zahner, Germany). The modified electrodes obtained via the above methods was used as the working electrode, a platinum wire (radius 0.5 mm) and an Ag/AgCl electrode were used as the auxiliary and reference electrode. The cyclic voltammetric measurements were taken in an unstirred electrochemical cell. Time−current curves were obtained by consequently adding H_2O_2 solution with a certain concentration into PB containing 1.0 mM HQ at −0.2 V after achieving a steady state current. A magnetic Teflon stirrer provided the convective transport during the amperometric measurements. To eliminate dissolved oxygen, all the solutions used above were bubbled with highly pure argon for 15 min before experiments, and then the argon atmosphere was kept over the solutions throughout the experiments.

2.7. Characterization. SEM images were taken on a Zeiss Supra 40 scanning electron microscope at an acceleration voltage of 5 kV.

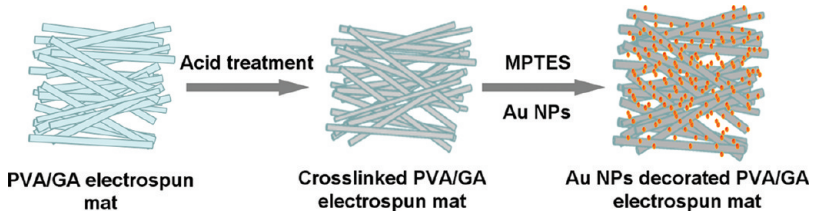

Figure 1. Schematic fabrication of water-stable functional Au NPs-PVA/GA electrospinning nanofibrous mats.

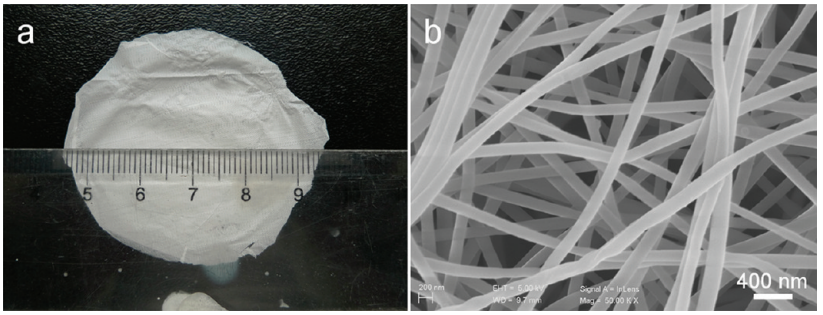

Figure 2. (a) Photograph and (b) SEM image of a freshly electrospun PVA/GA nanofibrous mat.

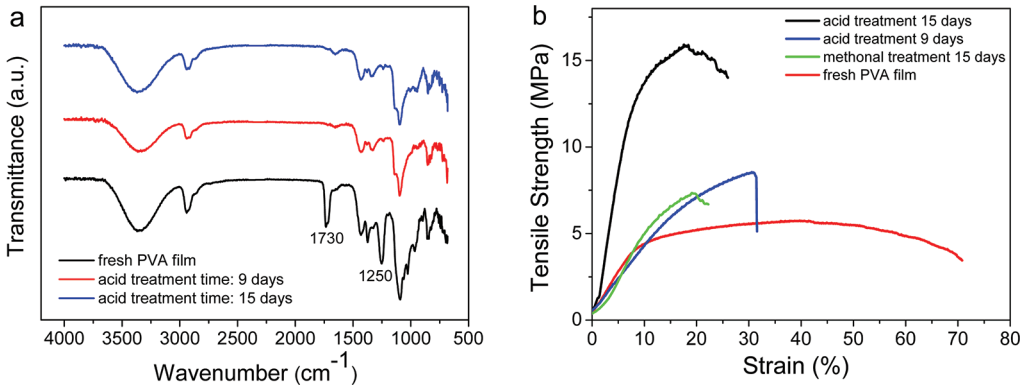

Figure 3. (a) IR spectra of cross-linked electrospun PVA/GA films after soaking in a mixed solution of HCl (37 wt %) aqueous solution (10 vol %) and methanol (90 vol %) with different time. (b) Typical stress−strain curves of the cross-linked PVA/GA electrospun film.

Transmission electron microscope (TEM) images were taken with a Hitachi H-7650 transmission electron microscope at an acceleration voltage of 120 kV. IR spectrum was obtained by a Magna-IR-750 spectrometer. The UV−vis spectra of the transparent films were collected on a Shimadzu DUV-3700. The mechanical properties of freestanding films were measured under tensile mode in a universal mechanical testing machine (Instron 5565 A) . For the mechanical testing, the PVA electrospun fibrous films were cut with a razor blade into rectangle bars of approximate length 20 mm and width 5 mm; the distance between the clamps was 7 mm, and the load speed was 10 mm min^{-1}. The resistance of Au NPs loaded PVA nanofibrous film was measured by digital multimeter. The distance between two probes was determined as 2 cm. In our cases, only when the density of the Au NPs shell covered on the PVA nanofiber increased to 537 mg(Au)/g(PVA), the Au NPs-PVA hybrid film became electrically conductive with the resistance of 2 kΩ. The resistance of the PVA nanofibrous film loading with lower densities of Au NPs cannot be measured.

3. RESULTS AND DISCUSSION

3.1. Fabrication of Water-Stable PVA Electrospun Nanofibrous Mats. Figure 1 shows the fabrication procedure of Au NPs modified water stable PVA nanofibrous mats. We first fabricated the water stable PVA electrospun fibrous mat by adopting *in situ* cross-linking in electrospun nanofibers. The solution containing both PVA and GA was electrospun into homogeneous nanofibers, and the electrospun PVA/GA nanofibers were immersed into acidic solution to promote the cross-linking occurred between hydroxyl groups of the PVA and the aldehyde groups of GA. The obtained cross-linked PVA/GA nanofibrous mat showed enhanced water resistant and mechanical properties compared with freshly prepared PVA/GA nanofibers without acidic treatment. Then, we modified the 3-mercaptopropyltrimethoxysilane (MPTES) on the surface of water-stable electrospun PVA fibrous mat to introduce thiol groups. Thus, gold nanoparticles (Au NPs) can be homogenously immobilized on the mat through a gold−sulfur bonding interaction after soaking the MPTES modified water stable electrospun PVA fibrous mat into a presynthesized citrate stabilized Au NPs solution. The densities of Au NPs decorated on the PVA fibrous mat can be controlled by changing the concentration of Au NPs aqueous solutions.

In the electrospinning process, the uniformity of electrospun PVA nanofibers is greatly influenced by the properties of polymer solution and the operating parameters. By adopting optimized experimental parameters (flow rate of 0.3 mL/h, voltage of 9 kV, collection distance of 17 cm, and polymer concentration of 8 wt %), we prepared a uniform PVA/GA nanofibrous mat with centimeter scale size (Figure 2a). The

dx.doi.org/10.1021/am300391j | ACS Appl. Mater. Interfaces 2012, 4, 1963−1971

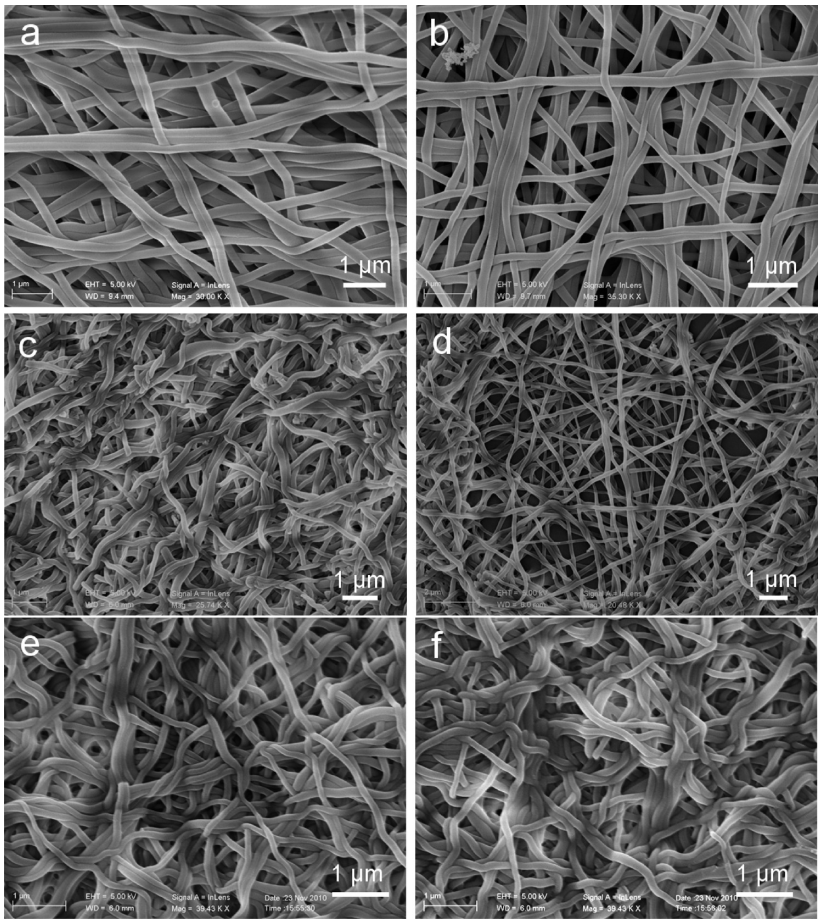

Figure 4. SEM images of cross-linked PVA electrospun nanofibrous mats before and after soaking in distilled water for desired time. (a and b) SEM images of the cross-linked PVA electrospun nanofibrous mats prepared by cross-linking for 9 days and 15 days, respectively, before soaking in water. (c and d) SEM images of the cross-linked PVA electrospun nanofibrous mats prepared by cross-linking for 9 days and 15 days, respectively, and then soaking in water for 4 h. (e and f) SEM images of the cross-linked PVA electrospun nanofibrous mats prepared by cross-linking for 9 days and 15 days, respectively, and then soaking in water for 24 h.

typical nanofibrous structure of the electrospun PVA/GA film was characterized by a scanning electron microscope (SEM). As Figure 2b shows, the obtained PVA/GA film was composed of nanofibers with a smooth surface, and the diameter of the PVA/GA electrospun nanofibers was narrowly distributed with a mean diameter of about 200 nm.

The prepared PVA/GA nanofibrous mats were soaked into a mixed solution of HCl and methanol to trigger the *in situ* cross-linking of PVA and GA in nanofibers. The occurrence of cross-linking in the nanofibrous mat was evidenced by Fourier trasform infrared (FTIR) spectroscopy (Figure 3a). A significant variation was observed in the FTIR spectra of PVA/GA electrospun films with prolonging immerged time in mixed solutions. The intensities of a strong adsorption peak at 1730 cm^{-1} assigned to the C═O stretching vibration of free GA aldehyde groups and the strong adsorption peak at 1250 cm^{-1} assigned to the C−O stretching vibration of hydroxyl groups in PVA decreased after the acidic treatment. This means that the H^+ provided by HCl promoted the cross-linking of the GA aldehyde groups and the PVA hydroxyl groups, leading to ether linkages.[43]

It is well known that the cross-linking of polymers would enhance their mechanical properties.[30,38] Thus, the tensile strengths of PVA/GA electrospun nanofibrous mats before and after acid induced *in situ* cross-linking were also measured to reflect the impact of the cross-linked role on the strength of PVA electrospun nanofibrous films. Typical stress−strain curves (Figure 3b) show that the tensile strength of nanofibrous mats with different cross-linked time. After acid-treatment for 9 days, the ultimate tensile strength of PVA/GA electrospun nanofibrous film increased from 6 to 9 MPa. The ultimate strain of a cross-linked PVA/GA electrospun film decreased to 40% compared with that (81%) of the fresh PVA electrospun nanofibrous film. The enhanced ultimate tensile strength and decrease of the ultimate tensile strain of acid-treatment PVA/GA electrospun film is ascribed to the cross-linking between the PVA and GA inside the fiber, which constructed a whole strong network. With increasing the immersion time in acid solutions to 15 days, the ultimate tensile strength of electrospun PVA nanofibrous film further increased to 16 MPa, accompanying with the decrease of ultimate tensile strain to 21%. This variation indicates that the longer immersion time will lead to more cross-linking points formed in PVA electrospun nanofibers. Additionally, the increase of crystalline degree of PVA induced by methanol is also a significant factor to enhance the tensile strength of electrospun PVA fibrous films.[19] The tensile strength of the PVA/GA electrospun film treated in methanol for 15 days was tested (Figure 3b). The result shows that after the methanol treatment, the film's ultimate tensile strength is 7 MPa, which

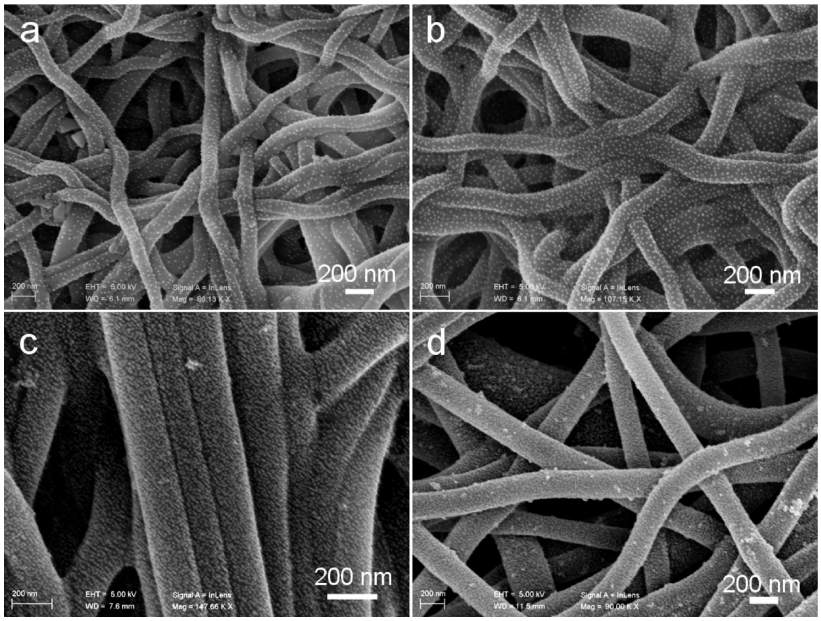

Figure 5. SEM images of Au NPs-PVA electrospun hybrid films with different mass concentration of Au NPs: (a) 53 mg(Au)/g(PVA), (b) 134 mg(Au)/g(PVA), (c) 268 mg(Au)/g(PVA), and (d) 537 mg(Au)/g(PVA).

is higher than the ultimate tensile strength of fresh PVA film but lower than that of acid treated PVA film. Obviously, both the acid triggered cross-linkage and crystallization of methanol contributed to the increase of the tensile strength of electrospun PVA nanofibrous film.

The water stabilities of PVA electrospun fibrous mats after cross-linking were investigated by the direct observation of morphological variation after soaking these mats in distilled water for the desired time. Figure 4 shows the SEM images of cross-linked PVA electrospun nanofibrous films before and after soaking in distilled water. The morphologies of the PVA electrospun nanofibrous films prepared by cross-linking for 9 days (Figure 4a) and 15 days (Figure 4b) are distinct nanofibers, although it seems a little buckled compared with the morphology of freshly prepared PVA electrospun nanofibrous mat (Figure 2b). After soaking these cross-linked PVA electrospun nanofibrous mats in distilled water for 4 h, the PVA electrospun nanofibers were swollen, became soft, and intertwined together (Figure 4c,d). Further extending the immersion time in water to 24 h, the nanofiber morphologies (Figure 4e,f) of cross-linked PVA electrospun fibers were still maintained in these mats indicating their water stabilities. The weight change of the PVA electrospun nanofibrous mat after immersing in water is tiny, implying the insolubility of cross-linked PVA nanofibers. Additionally, the morphologies of the PVA electrospun nanofibers prepared by cross-linking for 9 days and 15 days after soaking in distilled water are similar, which indicates that a longer cross-linked time than 9 days contributes little enhancement of water stability.

3.2. Decoration of Au NPs onto the Water-Stable PVA Electrospun Nanofibrous Mat. Considering the cross-linking time, the water-stable behavior, and mechanical properties, we chose the cross-linked PVA electrospun nanofibrous mat treated by acid for 9 days as the substrate material for Au NPs decoration. In order to immobilize Au NPs on the water stable PVA electrospun nanofibrous mat, the 3-mercaptopropyltrimethoxysilanes (MPTES) were first modified on the surface of water-stable PVA electrospun nanofibrous films to introduce thiol groups by soaking the PVA nanofibrous mat in MPTES ethanol solution for 10 h. The MPTES modified water stable PVA nanofibrous mats were then immersed into Au NPs aqueous solutions under shaking in an incubator shaker. Au NPs were tightly decorated onto the surface of PVA nanofibers by a strong affinity between the thiol group and Au NPs.

A series of Au NPs-PVA electrospun nanofibrous mats with a different mass concentration of Au NPs compared to PVA (mg(Au)/g(PVA)) were prepared. The homogeneous distributions of Au NPs decorated on surfaces of cross-linked PVA electrospun nanofibrous films were characterized by SEM. As Figure 5 shows, an obvious transformation of the PVA electrospun nanofiber surface from smooth to coarse appeared with increasing the mass concentration of Au NPs loaded on the water stable PVA electrospun nanofibers. When the mass concentration of Au NPs immobilized on the surface of cross-linked PVA electrospun nanofibrous mat was 53 mg(Au)/g(PVA), a few separated Au NPs can be observed on the surfaces of PVA nanofibers. Accompanied with the mass concentration of Au NPs increased from 53 mg(Au)/g(PVA) to 537 mg(Au)/g(PVA), the density of Au NPs attached on the surfaces of PVA nanofibers gradually increased and the distances among Au NPs decreased. Figure 5d shows that some Au NPs aggregates appeared on the PVA nanofibers. When the density of Au NPs shell covered on the PVA nanofiber increased to 537 mg(Au)/g(PVA), it seems that a dense Au NPs shell formed on the PVA nanofibers. Thus, the Au NPs-PVA hybrid film became electrically conductive with a resistance of 2 kΩ.

The color of Au NPs-PVA hybrid mats changed from deep purple to dusky golden with the increase of Au NPs densities on the surfaces of water stable PVA electrospun nanofibrous mats. The optical properties of Au NPs-PVA nanofibrous hybrid films with different densities of Au NPs were revealed by the UV−vis absorption spectra (Figure 6). Only one absorbance band with a maximum absorption at 520 nm was recorded on the Au NPs-PVA hybrid film of 53 mg(Au)/

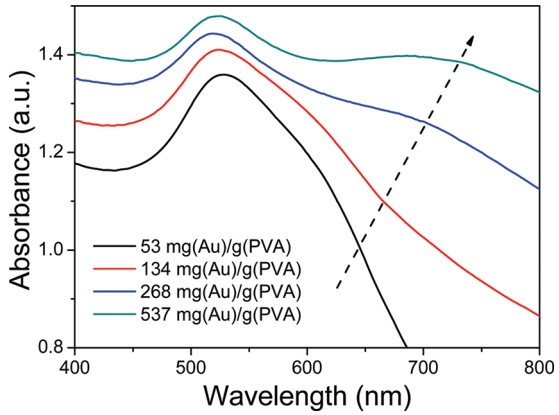

Figure 6. UV–vis absorption spectra of Au NPs-PVA electrospun nanofibrous hybrid films with different densities of Au NPs.

g(PVA), which is considered to be the plasmon resonance band of isolated spherical Au NPs.[44] It is worth noting that with the increase of Au NPs mass concentration on PVA nanofibrous mats, the other absorbance bands with absorption at about 750 nm beside the plasmon resonance band of isolated spherical Au NPs appeared, which is associated with the surface plasmon coupling between adjacent Au NPs.[45] Moreover, the new formed collective plasmon resonance band red-shifted with the increase of the number of Au NPs-immobilized on the surface of PVA electrospun nanofibers, indicating a higher densities of Au NPs and stronger aggregation state.

3.3. Application As Substrate Material of Biosensor for H_2O_2 Detection. As is shown above, we have fabricated the homogeneously distributed Au NPs-PVA hybrid nanofibrous films via a facile route. By combinational consideration of the flexible and portable properties of the PVA mat and biorelated functions of Au nanoparticles together, we believe that these fabricated Au NPs-PVA nanofibrous hybrid films can be used as efficient substrate materials integrated in biosensors. In order to demonstrate the function as biosensor substrate materials of the obtained Au-NPs/PVA hybrid mats, we set up biosensors for H_2O_2 detection by using these hybrid films. Hydrogen peroxide (H_2O_2) detection is important because it has practical applications in various fields such as food, clinical, pharmaceutical, industrial, biological, or environmental research areas. The high concentration of H_2O_2 will cause a negative effect on human health.

To detect the concentrations of H_2O_2, horseradish peroxidase (HRP) was usually used for the determination of H_2O_2 since HRP is an important peroxidase that contains iron heme prosthetic groups in their polypeptide pockets and can catalyze the oxidation of substrates when activated by hydrogen peroxide or other peroxides.[34] HRP could be attached tightly to the negatively charged Au NPs through electrostatic attraction due to its positive charge at pH values below its isoelectric point (the pH value at the isoelectric point is 8.9). Hydroquinone (HQ) is used to detect hydrogen peroxide as an excellent electron mediator.

The reaction sequence below shows a proposed reaction mechanism of the amperometric H_2O_2 biosensor and the effect of the electron mediator.

$$H_2O_2 + HRP(Red) \rightarrow HRP(Ox) + H_2O \quad (1)$$

$$HRP(Ox) + HQ \rightarrow BQ + HRP(Red) \quad (2)$$

$$BQ + 2H^+ + 2e^- \rightarrow HQ \quad (3)$$

HRP is oxidized by H_2O_2 in this reaction. The electron mediator, HQ, is then oxidized to benzoquinone (BQ), and the resulting BQ is reduced to HQ. The electrical current generated through these reactions is indicative of the presence of H_2O_2.[46] Figure 7 shows a schematic presentation of the hydrogen peroxide sensor based on the HRP/Au NPs–PVA/GCE.

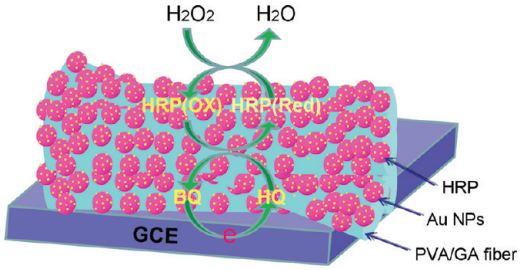

Figure 7. Schematic presentation of the hydrogen peroxide biosensor based on the HRP/AuNPs–PVA/GCE.

The electrochemical behavior of the HRP/PVA/GCE and HRP/Au NPs–PVA/GCE in the absence and presence of 5.0 mM of H_2O_2 was revealed by using cyclic voltammetry (Figure 8a,b). Aqueous solutions with 1.0 mM of HQ in 0.1 M of sodium phosphate buffer (PB) at pH 6.8 were used for the electrochemical measurement. Well-defined cyclic voltammograms (CVs) were observed in biosensors based on both the HRP/PVA/GCE and HRP/Au NPs–PVA/GCE (Figure 8a,b, curve I). The redox peak currents of HQ are about 32 and 28 μA, with potentials at (0.23 and −0.02 V) and (0.34 and −0.08 V), respectively. An obvious increase of the peak-to-peak separation was observed. This result confirmed that Au NPs successfully promoted the HRP embedded in the Au NPs–PVA nanofibrous films, and the presence of Au NPs had little effect on the interfacial electron-transfer kinetics of HQ at the electrode interface.[34]

In the presence of HQ and H_2O_2, the redox peak potential obtained at the HRP/PVA/GCE (Figure 8a, curve II) was (0.22 and −0.03 V). The presence of H_2O_2 had little effect on the reduction peak currents (37 μA) and the potential of HQ, indicating that there was weak reaction between HQ and H_2O_2.[34] While for HRP/Au NPs–PVA/GCE, the reduction current (102 μA) caused by HQ increased significantly accompanying with the disappearance of the oxidation current peak when 5.0 mM H_2O_2 was added (Figure 8b, curve II), suggesting that strong reactions among HRP, H_2O_2, and HQ existed. However, compared with the HRR/Au NPs–PVA/GCE, the HRP/PVA/GCE demonstrated much smaller electrocatalytic reduction peak currents toward H_2O_2 at the same concentration. The CVs indicate that the HRP/Au NPs–PVA/GCE shows an excellent electrochemical catalysis for H_2O_2, not just the simple combination effects of PVA films and Au NPs, which are probably due to the highly porous fibrous structure and increased surface area of Au NPs-PVA nanofibrous mats.

The electrochemical behavior of HRP/Au NPs–PVA/GCE with different mass concentration of Au NPs in the absence and presence of 5.0 mM of H_2O_2 was revealed by the cyclic voltammograms (Figure 9). When the mass concentration of Au NPs decorated on the PVA nanofibrous mat was 53 mg(Au)/g(PVA), the reduction current caused by HQ was

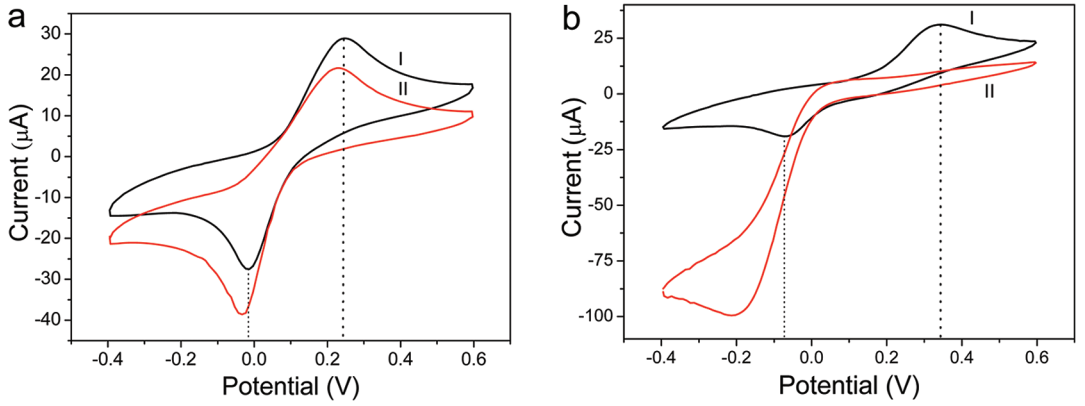

Figure 8. Cyclic voltammograms of 1.0 mM HQ in 0.1 M PB (pH 6.8) at (a) HRP/PVA/GCE, (b) HRP/Au NPs–PVA/GCE, in the absence (I) and presence (II) of 5.0 mM H_2O_2; scan rate, 100 mV s^{-1}.

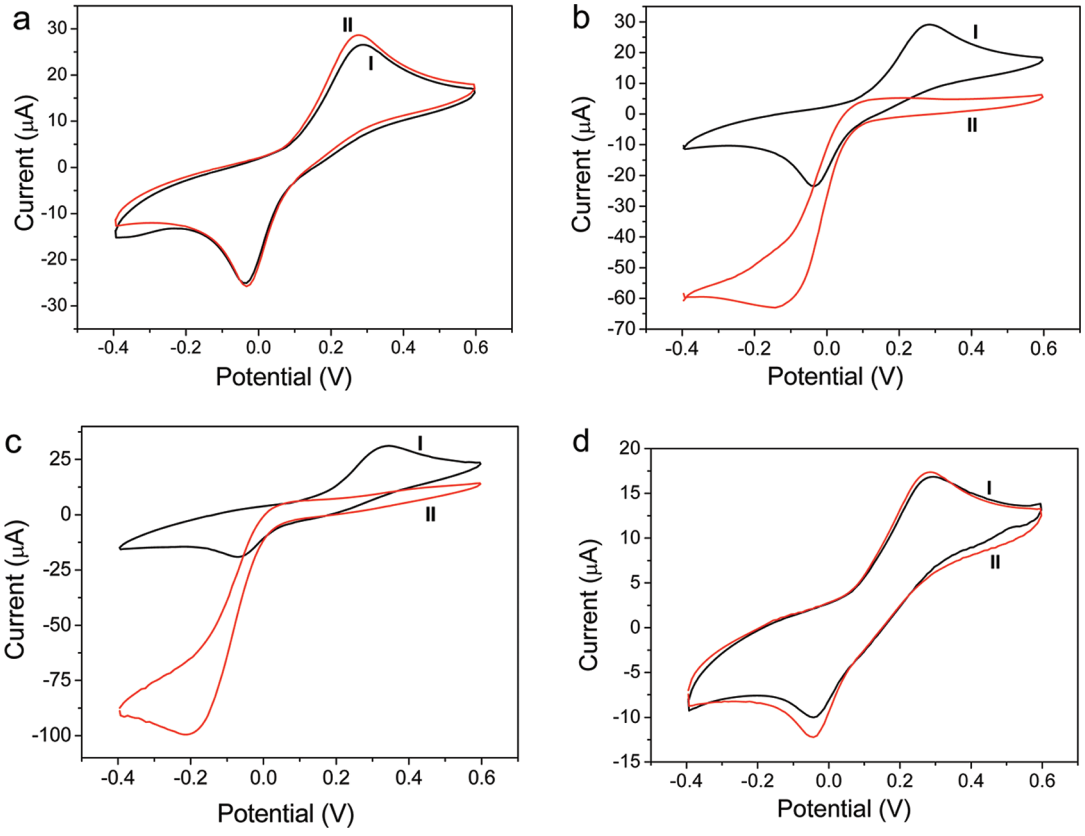

Figure 9. Cyclic voltammograms of 1.0 mM HQ in 0.1 M PB (pH 6.8) at the different densities of Au particles on PVA films in the absence (I) and presence (II) of 5.0 mM H_2O_2; scan rate, 100 mV s^{-1}: (a) 53 mg(Au)/g(PVA), (b) 134 mg(Au)/g(PVA), (c) 268 mg(Au)/g(PVA), and (d) 537 mg(Au)/g(PVA).

only 26 μA. With the mass concentration of Au NPs decorated on PVA nanofibrous mats increased to 134 mg(Au)/g(PVA) and then 268 mg(Au)/g(PVA), the reduction current caused by HQ increased significantly to 64 and 102 μA. However, with a further increase of the mass concentrations of Au NPs to 537 mg(Au)/g(PVA), the reduction current decreased to 14 μA. The fabricated HRP biosensor allowed the highly sensitive detection of H_2O_2, only the mass concentrations of Au NPs decorated on the electrospun PVA films were kept in a suitable range. With a small quantity of Au NPs loaded on the mat, the active surface area for reactions among HRP, H_2O_2, and HQ on the Au NPs–PVA nanofibrous hybrid mat was insufficient leading to a low response to H_2O_2. Additionally, the low concentration of Au NPs on PVA nanofibers means low efficiency electron transfer in Au-PVA hybrid films, which also results in low response to H_2O_2. However, if the density of Au NPs on the surface of the PVA electrospun nanofibrous mats is too high, the active sites were also blocked due to the agglomeration of Au NPs. Thus, the sensitivity to H_2O_2 of the sensors fabricated by the high-density Au NPs-PVA nanofibrous film is low.

Considering the good reduction current (102 μA) caused by HQ in the presence of H_2O_2, we choose the Au NPs-PVA hybrid nanofibrous mat of 268 mg(Au)/g(PVA) as the substrate material to accurately determine the concentration of H_2O_2. Figure 10a shows the amperometry response and

dx.doi.org/10.1021/am300391j | ACS Appl. Mater. Interfaces 2012, 4, 1963–1971

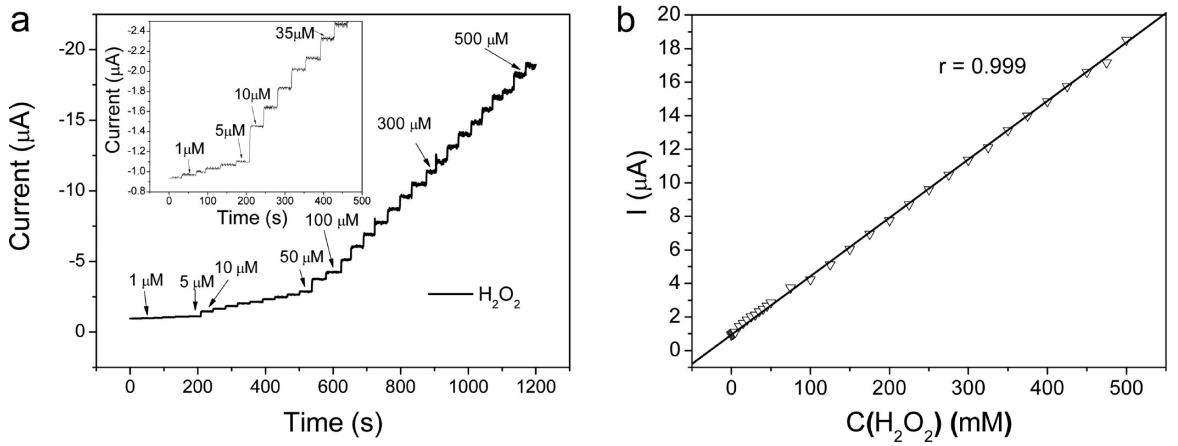

Figure 10. (a) Amperometric response of the fabricated HRP/Au NPs−PVA/GCE biosensor to successive addition of H_2O_2 into the stirred PBS solution (0.1 M, pH 6.8) containing 1.0 mM HQ, the applied potential was −0.2 V vs Ag/AgCl, and (b) calibration curve and linear fitting curve between the current and the H_2O_2 concentration.

calibration curve of steady state current vs concentration of H_2O_2. Stepped increases of the amperometric reduction currents were observed with the addition of H_2O_2 at a constant potential of −0.2 V (Figure 10a). The current response of the sensors was rapidly enhanced and approached about 98% of its steady state current within 1 s. The response time is much shorter than 35, 15, 2, and 2 s obtained at the HAP-Nafion-silica sonogel carbon composite electrode,[47] HRP/Au colloid/cysteamine modified electrode,[48] HRP−HAP/GC electrode,[39] and CAT/nano Fe_3O_4/Au electrode,[49] respectively. These results suggest that the rapid electrode response to the change of the H_2O_2 concentration is due to the fast diffusion of the H_2O_2 into the Au NPs-PVA nanofibrous network structures.

The obvious increase of the reduction current can be observed when the concentration of H_2O_2 was as low as 1 μM (inset picture in Figure 10a) for HRP/Au NPs−PVA/GCE. The amperometry result indicates that the HRP/Au NPs−PVA/GCE exhibits high sensitivity. The current responses showed a linear relationship with the concentration of H_2O_2 (1 μM to 0.5 mM) with the correlation coefficient of 0.999 (n = 32) as shown in Figure 10b. The linear range is wider than those obtained at the HRP-Au NP-TiO_2 nanotube arrays modified electrode (5 μM to 0.4 mM),[50] HRP-mesoporous silica hollow sphere-Nafion/GC electrode (3.9 μM to 0.14 mM),[40] HAP-Nafion-silica sonogel-carbon composite electrode (4 μM to 0.1 mM),[47] and CAT/nano Fe_3O_4/Au electrode (1.5 μM to 13.5 μM).[49] The detection limit was 0.5 μM H_2O_2 determined from the linear graph (signal-to-noise ratio = 3), which is comparable to that obtained at the HRP−Fe_3O_4/m-silica nanoparticles modified electrode (0.47 μM)[46] and CAT/nano Fe_3O_4/Au electrode (0.5 μM),[49] better than those obtained at the Au NPs−$CaCO_3$/silica sol−gel (1 μM),[51] HAP-a-zirconium phosphate/GC electrode (1.2 μM),[41] HRP-nano-Au-carbon ceramic electrode (6.1 μM),[52] and HRP-DNA/GC electrode (25 μM).[53] The comparison of response time, detection range, and detection time of different H_2O_2 detection biosensors was summarized in Table 1, indicating that the as-prepared Au−PVA hybrid nanofibrous mat can be used as a substrate material for the development of enzyme-based amperometric biosensors for H_2O_2 detection.

Table 1. Summary of the Response Time, Detection Range, and Detection Time of As-Prepared H_2O_2 Detection Sensors in Comparison with Other Reported Sensors

biosensors	response time (s)	detection range (μM)	detection limit (μM)	ref
HRP-Au NPs-PVA NFs	1	1−500	0.5	this work
HRP-Au NPs-cellulose NFs	1	1−500	1	34
HRP-HAP NPs	2	5−820	0.1	39
HRP-Fe_3O_4-silica	no data	2−24	0.43	46
HRP-sonogel-carbon	no data	4−100	1.6	47
CTA-Fe_3O_4-Au NPs	2	1.5−13.5	0.5	49
HRP -TiO_2 NTs-Au NPs	5	5−400	2	50
HRP-Au NPs-$CaCO_3$-silica	no data	40−8000	1	51
HRP-Au NPs-carbon	8	12.2−1100	6.1	52

4. CONCLUSIONS

In summary, we developed a facile way to prepare a Au NPs homogeneously modified cross-linked PVA electrospun nanofibrous mat and showed its application as an efficient substrate material to fabricate biosensors for H_2O_2 detection. The water stable and robust PVA nanofibrous mat was first prepared via the electrospinning process combining the *in situ* cross-linked in PVA nanofibers. Then, Au NPs were homogeneously decorated on the PVA nanofibrous mat through the linkage role of MPTES. The obtained Au NPs-PVA hybrid nanofibrous film with the Au NPs density of 268 mg(Au)/g(PVA) have been demonstrated as an efficient substrate material for biosensors to detect H_2O_2. The fabricated HRP biosensor allowed the highly sensitive detection of H_2O_2 with a detection limit of 0.5 μM and exhibited a fast response, broad linear range, and low detection limit. The feasible process and high detection sensitivity of the biosensor based on Au NPs modified PVA electrospun nanofibrous mats may pave the way in developing new a film support-enzyme hybrid substrate material for biosensors or bioelectrocatalysts.

AUTHOR INFORMATION

Corresponding Author

*Fax: + 86 551 3603040. E-mail: shyu@ustc.edu.cn.

Notes

The authors declare no competing financial interest.

ACKNOWLEDGMENTS

This work is supported by the National Basic Research Program of China (Grant 2010CB934700), the National Natural Science Foundation of China (Grants 91022032, 21061160492, and J1030412), International Science & Technology Cooperation Program of China (Grant 2010DFA41170), and the Principal Investigator Award by the National Synchrotron Radiation Laboratory at the University

REFERENCES

(1) Chen, L.; Bromberg, L.; Lee, J. A.; Zhang, H.; Schreuder-Gibson, H.; Gibson, P.; Walker, J.; Hammond, P. T.; Hatton, T. A.; Rutledge, G. C. *Chem. Mater.* **2010**, *22*, 1429.

(2) He, D.; Hu, B.; Yao, Q.-F.; Wang, K.; Yu, S.-H. *ACS Nano* **2009**, *3*, 3993.

(3) Krogman, K. C.; Lowery, J. L.; Zacharia, N. S.; Rutledge, G. C.; Hammond, P. T. *Nat. Mater.* **2009**, *8*, 512.

(4) Li, D.; Xia, Y. N. *Adv. Mater.* **2004**, *16*, 1151.

(5) Greiner, A.; Wendorff, J. H. *Angew. Chem., Int. Ed.* **2007**, *46*, 5670.

(6) Lu, X.; Wang, C.; Wei, Y. *Small* **2009**, *5*, 2349.

(7) Schiffman, J. D.; Schauer, C. L. *Polym. Rev.* **2008**, *48*, 317.

(8) Wu, H.; Hu, L.; Rowell, M. W.; Kong, D.; Cha, J. J.; McDonough, J. R.; Zhu, J.; Yang, Y.; McGehee, M. D.; Cui, Y. *Nano Lett.* **2010**, *10*, 4242.

(9) Thavasi, V.; Singh, G.; Ramakrishna, S. *Energy Environ. Sci.* **2008**, *1*, 205.

(10) Dai, Y.; Liu, W.; Formo, E.; Sun, Y.; Xia, Y. *Polym. Adv. Technol.* **2011**, *22*, 326.

(11) Gopal, R.; Kaur, S.; Ma, Z.; Chan, C.; Ramakrishna, S.; Matsuura, T. *J. Membr. Sci.* **2006**, *281*, 581.

(12) Yun, K. M.; Hogan, C. J. Jr.; Matsubayashi, Y.; Kawabe, M.; Iskandar, F.; Okuyama, K. *Chem. Eng. Sci.* **2007**, *62*, 4751.

(13) Lee, J. A.; Krogman, K. C.; Ma, M.; Hill, R. M.; Hammond, P. T.; Rutledge, G. C. *Adv. Mater.* **2009**, *21*, 1252.

(14) Pham, Q. P.; Sharma, U.; Mikos, A. G. *Tissue Eng.* **2006**, *12*, 1197.

(15) Sill, T. J.; von Recum, H. A. *Biomaterials* **2008**, *29*, 1989.

(16) Wang, X.; Kim, Y.-G.; Drew, C.; Ku, B.-C.; Kumar, J.; Samuelson, L. A. *Nano Lett.* **2004**, *4*, 331.

(17) Kowalczyk, T.; Nowicka, A.; Elbaum, D.; Kowalewski, T. A. *Biomacromolecules* **2008**, *9*, 2087.

(18) Patel, A. C.; Li, S.; Yuan, J.-M.; Wei, Y. *Nano Lett.* **2006**, *6*, 1042.

(19) Yao, L.; Haas, T. W.; Guiseppi-Elie, A.; Bowlin, G. L.; Simpson, D. G.; Wnek, G. E. *Chem. Mater.* **2003**, *15*, 1860.

(20) Ding, B.; Kim, H.-Y.; Lee, S.-C.; Shao, C.-L.; Lee, D.-R.; Park, S.-J.; Kwag, G.-B.; Choi, K.-J. *J. Polym. Sci., Part B: Polym. Phys.* **2002**, *40*, 1261.

(21) Zeng, J.; Hou, H.; Wendorff, J. H.; Greiner, A. *Macromol. Rapid Commun.* **2005**, *26*, 1557.

(22) Keun Son, W.; Ho Youk, J.; Seung Lee, T.; Park, W. H. *Mater. Lett.* **2005**, *59*, 1571.

(23) Koski, A.; Yim, K.; Shivkumar, S. *Mater. Lett.* **2004**, *58*, 493.

(24) Naebe, M.; Lin, T.; Staiger, M. P.; Dai, L.; Wang, X. *Nanotechnology* **2008**, *19*, 305702.

(25) Wang, X.; Chen, X.; Yoon, K.; Fang, D.; Hsiao, B. S.; Chu, B. *Environ. Sci. Technol.* **2005**, *39*, 7684.

(26) Zeng, J.; Hou, H.; Wendorff, J. H.; Greiner, A. *e-Polym.* **2004**, No. 78.

(27) Brasch, U.; Burchard, W. *Macromol. Chem. Phys.* **1996**, *197*, 223.

(28) Wu, L.; Yuan, X.; Sheng, J. *J. Membr. Sci.* **2005**, *250*, 167.

(29) Tang, C.; Saquing, C. D.; Harding, J. R.; Khan, S. A. *Macromolecules* **2009**, *43*, 630.

(30) Xiao, S.; Shen, M.; Guo, R.; Huang, Q.; Wang, S.; Shi, X. *J. Mater. Chem.* **2010**, *20*, 5700.

(31) Boisselier, E.; Astruc, D. *Chem. Soc. Rev.* **2009**, *38*, 1759.

(32) Han, G.; You, C.-C.; Kim, B.-j.; Turingan, R. S.; Forbes, N. S.; Martin, C. T.; Rotello, V. M. *Angew. Chem., Int. Ed.* **2006**, *45*, 3165.

(33) Cui, R.; Liu, C.; Shen, J.; Gao, D.; Zhu, J.-J.; Chen, H.-Y. *Adv. Funct. Mater.* **2008**, *18*, 2197.

(34) Zhang, T.; Wang, W.; Zhang, D.; Zhang, X.; Ma, Y.; Zhou, Y.; Qi, L. *Adv. Funct. Mater.* **2010**, *20*, 1152.

(35) Dong, H.; Fey, E.; Gandelman, A.; Jones, W. E. *Chem. Mater.* **2006**, *18*, 2008.

(36) Han, G. Y.; Guo, B.; Zhang, L. W.; Yang, B. S. *Adv. Mater.* **2006**, *18*, 1709.

(37) Demir, M. M.; Gulgun, M. A.; Menceloglu, Y. Z.; Erman, B.; Abramchuk, S. S.; Makhaeva, E. E.; Khokhlov, A. R.; Matveeva, V. G.; Sulman, M. G. *Macromolecules* **2004**, *37*, 1787.

(38) Fang, X.; Ma, H.; Xiao, S.; Shen, M.; Guo, R.; Cao, X.; Shi, X. *J. Mater. Chem.* **2011**, *21*, 4493.

(39) Zhang, H.; Li, C. Y.; Wu, P.; Gong, Z. N.; Xu, G. L.; Cai, C. X. *Analyst* **2011**, *136*, 1116.

(40) Sun, L. X.; Cao, Z. X.; Zhang, J.; Zeng, J. L.; Xu, F.; Cao, Z.; Zhang, L.; Yang, D. W. *Talanta* **2009**, *77*, 943.

(41) Yang, W. S.; Yang, X. S.; Chen, X.; Yang, L. *Bioelectrochemistry* **2008**, *74*, 90.

(42) Frens, G. *Nat. Phys. Sci.* **1973**, *241*, 20.

(43) Tang, C.; Saquing, C. D.; Harding, J. R.; Khan, S. A. *Macromolecules* **2010**, *43*, 630.

(44) Puntes, V.; Ojea-Jimenez, I. *J. Am. Chem. Soc.* **2009**, *131*, 13320.

(45) Yang, Y.; Matsubara, S.; Nogami, M.; Shi, J. L.; Huang, W. M. *Nanotechnology* **2006**, *17*, 2821.

(46) Won, Y.-H.; Aboagye, D.; Jang, H. S.; Jitianu, A.; Stanciu, L. A. *J. Mater. Chem.* **2010**, *20*, 5030.

(47) de Cisneros, J. L. H. H.; Elkaoutit, M.; Naranjo-Rodriguez, I.; Dominguez, M.; Hernandez-Artiga, M. P.; Bellida-Milla, D. *Electrochim. Acta* **2008**, *53*, 7131.

(48) Chen, H. Y.; Xiao, Y.; Ju, H. X. *Anal. Biochem.* **2000**, *278*, 22.

(49) Thandavan, K.; Gandhi, S.; Sethuraman, S.; Rayappan, J. B. B.; Krishnan, U. M. *Nanotechnology* **2011**, *22*, 265505.

(50) Chen, A.; Kafi, A. K. M.; Wu, G. *Biosens. Bioelectron.* **2008**, *24*, 566.

(51) Zhu, J. H.; Cai, W. Y.; Xu, Q.; Zhao, X. N.; Chen, H. Y. *Chem. Mater.* **2006**, *18*, 279.

(52) Lei, C. X.; Hu, S. Q.; Gao, N.; Shen, G. L.; Yu, R. Q. *Bioelectrochemistry* **2004**, *65*, 33.

(53) Luo, S. L.; Zeng, X. D.; Li, X. F.; Liu, X. Y.; Liu, Y.; Kong, B.; Yang, S. L.; Wei, W. Z. *Biosens. Bioelectron.* **2009**, *25*, 896.